J Nanopart Res (2011) 13:1573–1580
DOI 10.1007/s11051-010-9908-3

RESEARCH PAPER

Antibody immobilization on gold nanoparticles coated layer-by-layer with polyelectrolytes

Bernard Masereel · Mustapha Dinguizli · Caroline Bouzin · Nicolas Moniotte · Olivier Feron · Bernard Gallez · Thierry Vander Borght · Carine Michiels · Stéphane Lucas

Received: 27 October 2009 / Accepted: 17 March 2010 / Published online: 2 April 2010

Abstract Nanoscale materials are used in the biomedical field for magnetic resonance imaging, protein detection and drug/gene delivery. Gold nanoparticles (AuNPs) are particularly investigated in cancer treatment and imaging. In this study, we described a simple and reliable liquid method to coat AuNPs (diameter: 21 nm) layer-by-layer with alternative cationic polyallylamine and anionic polystyrenesulfonate. The C-terminal amino acid of the antibody directed against anti-bovine serum albumin was activated by EDC/NHS, and then condensed with the amino functions of the external polyallylamine layer. An ELISA test confirmed that the antigen recognition of the bioconjugate antibody was conserved. This AuNP coating and the covalently coupling could be used as a generic process for binding other specific antibodies, particularly those overexpressed in cancer cells and angiogenesis.

Keywords Gold · Nanoparticles · Polymer · Antibody · Polyallylamine · Polystyrenesulfonate · Nanomedicine · Drug delivery

B. Masereel (✉) · M. Dinguizli · N. Moniotte
Drug Design and Discovery Center, FUNDP, University of Namur, Namur, Belgium
e-mail: bernard.masereel@fundp.ac.be

C. Bouzin · O. Feron · B. Gallez
Pole of Pharmacology and Therapeutics, University of Louvain, Louvain, Belgium

T. Vander Borght
Mont-Godinne Hospital, University of Louvain, Louvain, Belgium

C. Michiels
Department of Biology, FUNDP, University of Namur, Namur, Belgium

S. Lucas
Research Center in Physics of Matter and Radiation, FUNDP, University of Namur, Namur, Belgium

Introduction

In the past decade, nanoparticles technology has become a major field of investigation in colloid and material science leading to various applications especially in the biomedical field (Bawarski et al. 2008) such as magnetic resonance imaging (Artemov et al. 2003), protein detection (Cao et al. 2003; Bucak et al. 2003), drug/gene delivery (Forbes et al. 2003), and cancer treatment (Fortina et al. 2007). The immobilization of organic molecules (proteins, DNA,…) on nanoparticles allows the formation of conjugate materials which make it possible to combine two or more desirable properties. Molecules can be immobilized on a carrier either passively through hydrophobic or ionic interactions (physical adsorption), or covalently by linking an activated surface group. Immobilization by covalent coupling provides a number of distinct advantages over physical adsorption such as a higher stability of the bioconjugate (Wilson and Nock 2002).

Covalent immobilization of proteins requires nanoparticles with activated chemical groups that are able to react with primary amines or carboxylic acids, the two most available groups on the protein surface. Polymer coating of nanoparticles is one method to modify surface properties where the most external polymer type determines the final surface features of the coated nanoparticle. Early studies on the polymer modification of the nanoparticle surface focused on chemisorption or adsorption of a preformed polymer, or deposition by in situ polymerization (suspension, emulsion, or vapor phase) (Hofman-Caris 1994). However, the coating of nanoscale objects proves to be very difficult due to the stability of the nanoparticles in suspension during and after the coating process.

A major area of polymer coating uses polyelectrolytes to modify colloids by using electrostatic attraction for auto-assembling deposition (Gittins and Caruso 2001). Polyelectrolytes present many advantages over other techniques and uncharged polymers. First, they can be deposited layer-by-layer (LbL) onto the nanoparticle surface where the shell thickness is related to the number of layers (Decher 1997). Indeed, the LbL approach uses two solutions of oppositely charged polymers into which the surface is dipped (or colloid is diluted depending on the substrate) (Caruso 2001). Once deposited, the first layer of polyelectrolyte inverts the surface charge. So, a second polyelectrolyte bearing opposite charges can be deposited. The repetition of this process allows the formation of homogenous multilayer films. The LbL deposition has been widely used on various substrates but only a few publications report the deposition on nanoparticles (Gittins and Caruso 2000). Second, polyelectrolyte deposition can be achieved in aqueous media which is a prerequisite for many biomedical applications. Although very easy and quick, this technique is now recognized as a low cost and environmentally friendly technology. Third, charged nanoparticles tend to repeal each other, thus, allowing the preparation of highly stable particle suspensions (Mayya et al. 2003). This advantage is clearly important for further applications and covalent binding to biomolecules.

The purpose of this study is to highlight the advantage and the interest of polyelectrolytes for coating and functionalizing gold nanoparticles (AuNPs) by introducing reactive functions for covalent linking with antibodies which can specifically target cancer cells. Thus, the coupling of AuNPs to antibodies targeting surface proteins specifically overexpressed in cancer cells or in angiogenesis is an attractive challenge for the treatment of cancer. In this study, we LbL coated AuNPs alternatively with cationic polyallylamine (PAA) and anionic polystyrenesulfonate (PSS) (Fig. 1). The opposite charges of both polyelectrolytes stabilize the AuNP shell. AuNPs have a surface plasmon band very sensitive to environment changing, which allow controlling the growth of multilayer polyelectrolytes deposition. In this study, some of the cationic amino functions of the last external PAA layer are embedded into the underlying anionic PSS layer whereas other amino groups point at the surrounding AuNP medium. These last amino moieties are then condensed with the activated carboxylic function of the C-terminal amino acid of immunoglobulin.

The low-cost anti-bovine serum albumin immunoglobulin (anti-BSA IgG) was chosen to be linked to coated AuNPs. This concept could be also further applied to other monoclonal IgG antibodies whose use is widespread in various clinical diagnosis or treatment (Maggon 2007; Baptista et al. 2008), and in the development of biosensors (Buijs et al. 1995; Radwan and Azzazy 2009).

Materials and methods

AuNP coating by polyelectrolytes

The LbL AuNP coating was realized as reported by Schneider and Decher (2004). Typically, 180.0 mg of PAA (15 kDa, Aldrich, Benelux) was dissolved in 9.0 mL of ultrapure water and the solution was sonicated for 20 min. To discard sodium azide and sodium citrate used as preservative and stabilizer, respectively, the commercially available AuNP colloidal suspension (0.01% $HAuCl_4$, ø ~ 25 nm, Aldrich, Benelux) was washed by centrifugation (16,000*g*; 1.5 h). The supernatant was discarded and replaced by the same volume of ultrapure water. This AuNP solution (9 mL) was added dropwise under vigorous stirring to the PAA solution. Then, the mixture was gently stirred for 12 h in the dark. To remove the excess polymer, the monolayered AuNP suspension was washed three times by centrifugation (3 min at 10,000*g*; 5 min at 12,000*g* and 15 min at 13,000*g*). The second layer deposition was performed exactly

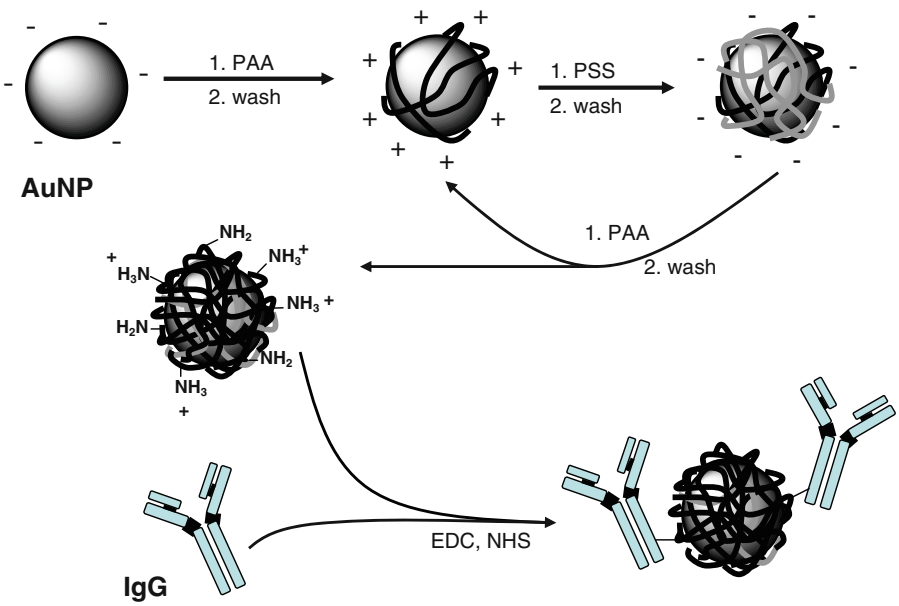

Fig. 1 Layer-by-layer coating of gold nanoparticles (AuNPs) with cationic polyallylamine (PAA) and anionic polystyrene-sulfonate (PSS) followed by immunoglobulin (IgG) linking through an amide bound. Coupling reagents: *EDC* ethyl-aminopropyl carbodiimide, *NHS N*-hydroxysuccinimide

according to the previous conditions where PAA was replaced by PSS (15 kDa, Bester, The Netherlands). In total, up to five layers can be deposited with the following sequence: AuNP/PAA/PSS/PAA/PSS/PAA. At the last purification cycle, the supernatant was discarded and replaced by HCl–Tris buffer (pH 8.2), and the suspension stored at 4 °C.

After coating, the ultraviolet spectrum (200–800 nm) of the AuNP suspension was recorded with a UV/Vis spectrophotometer (Perkin Elmer Lambda 20) to determine the peak of the gold plasmon band. On the other hand, zeta (ζ) potential of naked and coated AuNPs was measured at 25 °C with a Malvern Nano ZS (Malvern Instruments, UK). The instrument was calibrated with standard latex nanoparticles (Malvern Instruments, UK). Finally, a sample of the AuNP colloidal solution (9 μL) was also dropped on a TEM copper grid and dried before adding 7 μL of uranyl acetate 2% (p/v). Grids were observed with a TEM (Tcnaï 10 microscope) at 100 keV.

Mouse anti-BSA IgG binding to coated AuNP

Lyophilized mouse anti-BSA antibody (Raybiotech, USA) was diluted in phosphate buffer saline (1 mg mL^{-1}). This stock solution was further diluted with a carbonate buffer (pH 8.7; 5.0 mM). An equimolar aqueous solution of 1-ethyl-aminopropyl-carbodiimide (EDC, Aldrich, Benelux) and *N*-hydroxysuccinimide (NHS, Aldrich, Benelux) was prepared and added to the diluted solution of IgG. The EDC/NHS/IgG ratio was 1:1:1. Immediately, 10 μL of the IgG solution containing EDC and NHS were added to 490 μL of a solution of coated AuNPs (AuNP/PAA/PSS/PAA), and the mixture was stirred for 2 h. The final concentration of anti-BSA IgG was 1, 2, or 4 ng mL^{-1}. The IgG linked coated AuNP suspension was then washed three times by centrifugation (3 min at 10,000*g*; 5 min at 12,000*g*, and 15 min at 13,000*g*) to give 500 μL of anti-BSA IgG linked to AuNP/PAA/PSS/PAA. To avoid a covalent linking, the same procedure was performed without addition of EDC/NHS. In this case, the anti-BSA monoclonal antibody is only adsorbed on the three layered AuNPs.

ELISA test and gold dosage

The activity of anti-BSA IgG linked or adsorbed to coated AuNPs was determined by conventional ELISA. 96-well plates (Reacti-Bind, Thermo Scientific) were coated overnight at room temperature with 50 μg mL^{-1} BSA fraction V (Affymetrix). Coating was carried out using a dedicated buffer (AbD Serotec). Anti-BSA antibodies (Raybiotech, USA)

and bio-conjugates were incubated overnight at 4 °C in PBS containing Tween 20 (0.05%, w/v). After washing, specific hybridization was measured with a peroxidase-conjugated anti-mouse IgG antibody (Jackson Immunoresearch, 1:10,000 dilution in PBS containing 0.05% Tween 20) and addition of 3,3′,5,5′-tetramethylbenzidine as peroxidase substrate (TMB, Calbiochem). Plates were read at 450 nm with a VictorX4 microplate reader.

Gold dosage was performed on a Philips PU9200X spectrophotometer equipped with a gold hollow-cathode lamp. $HAuCl_4$ (SMI-Labhut Ltd) was used as standard for calibration (0.1–5 ppm). The supernatant of each well was poured off, and NaOH 2 M (100 µL) was added to hydrolyze proteins. Two hours later, a mixture of concentrated H_2SO_4 and HNO_3 (50:50) was added and refluxed (80 °C, 3 h) to dissolve AuNPs. The solution was diluted with water, and the gold concentration was measured by AAS.

Results

AuNP coating

Observed in TEM, a typical naked AuNP (as received in sodium citrate and azide solution) is shown in Fig. 2a. A three- and a five-layered AuNPs are shown on Fig. 2b, c, respectively. Their structure is AuNP/PAA/PSS/PAA and AuNP/PAA/PSS/PAA/PSS/PAA. As observed, the polymer shell thickness increases with the number of deposited layers. For 3- or 5-layered AuNPs, no aggregation is observed on the TEM grid, even after drying (Fig. 2d). The TEM analysis also revealed that AuNPs are individually coated. Statistical analysis of TEM grids allow the calculation of the number of individual (80%), double (15%) and aggregated (5%) AuNPs. Experiments by Schneider and Decher report similar results (Schneider and Decher 2004).

The size of coated AuNPs has been determined by measuring the diameter of whole particles on TEM images. As expected, the coated AuNP diameter grows with the number of deposited layers (Fig. 3). This is consistent with the literature where a linear dependence of the thickness on the number of layers was described (Toda et al. 2008). The uncoated AuNPs have an average size of 21.3 nm (±2.1 nm) which is in accordance with the mean value claimed by the provider (25 nm). Each polyelectrolyte layer increases the diameter by about 1.5 to 24.0 nm (±2.0 nm) for AuNP/PAA/PSS/PAA and 29.7 nm (±2.6 nm) for AuNP/PAA/PSS/PAA/PSS/PAA. Similar thickness increments were reported for a PAA/PSS bilayer coating SiOx (3.0 nm) and Au (2.9–4.1 nm), respectively (Toda et al. 2008; Caruso et al. 1997).

Spectral data of coated AuNPs with an increasing number of layers are shown in Fig. 4. A redshift of the gold plasmon band occurs for the first three layers deposited. The shift shows that the polymers do not remain in solution but really adsorb onto the surface of the colloids and produce small changes in the local refractive index that converts into spectral shifts in the extinction and scattering spectra. Indeed this band is influenced by the dielectric constant of the surrounding medium (Mulvaney 1996). Up to three layers, the gold plasmon band shift to the red. Over three layers, the plasmon band wavelength is stable due to a permanent change in the local refractive index (Khlebtsov and Dykman 2010).

During the coating process, the AuNPs do not precipitate or aggregate whatever the number of deposited layers. The stability of this colloidal suspension is crucial for further protein or IgG linking.

Zeta potential measurements of coated AuNPs confirmed the presence of an external cationic PAA or anionic PSS layer. Indeed the zeta potential value alternates according to the last adsorbed outer layer. Zeta potential values (+50 to +55 mV) are positive when the external layer is PAA whereas negative values are found for washed and naked AuNPs (-40 mV) or when PSS constitutes the external coating (−39 and −42 mV) (Table 1). These values are similar to those described by Dirieh Egueh et al. (2010) for these polymers.

IgG linking to coated AuNPs

To link IgG to coated AuNPs through an amide bond, an external PAA layer was required. As the preparation and the purification process of AuNP/PAA/PSS/PAA/PSS/PAA are more time consuming than those used for AuNP/PAA/PSS/PAA, the three-layered AuNP was selected and used for linking to the anti-BSA IgG monoclonal antibody. The C-terminal carboxylic function of the antibody was activated by EDC/NHS and condensed on the amine moiety of the external PAA layer of coated AuNPs (Fig. 1). The anti-BSA

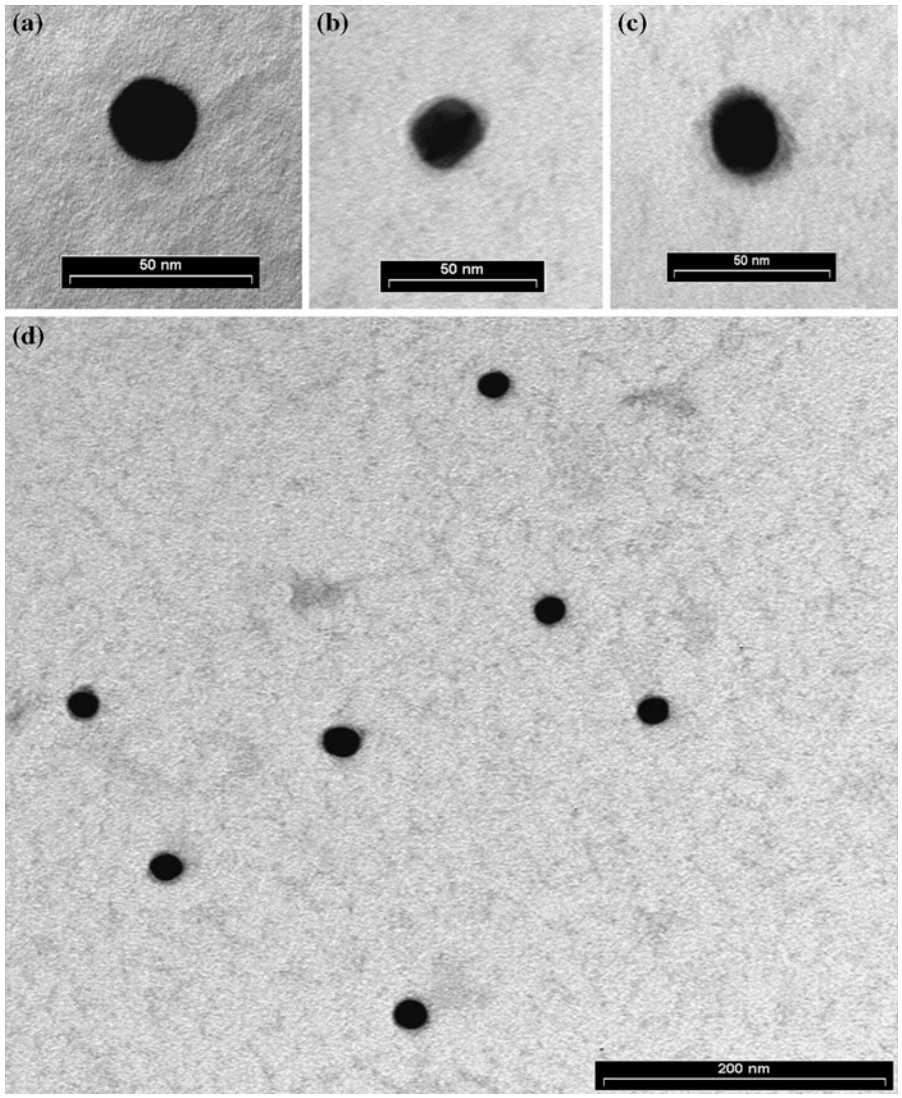

Fig. 2 Transmission Electron Microscopy of individual AuNPs before coating (**a**), after deposition of three (**b**) and five (**c**) layers. Isolated 3-layers AuNPs at lower magnification (**d**)

IgG was used at a concentration of 1, 2, or 4 ng/mL. The preparation was washed three times by centrifugation and assayed to confirm the reactivity of the antibody toward a specific secondary antibody coupled to horseradish peroxidase. When the linking reaction occurs, the ELISA response is linear and significantly related to the increase of the antibody concentration ($p < 0.01$) (Fig. 5). This confirms the specific hybridization of the AuNP-anti-BSA with BSA.

The same binding process was repeated in the same conditions, but without addition of EDC/NHS to prevent a covalent binding. The mixture was also washed three times or only twice, and then assayed by the same ELISA protocol. The ELISA response of the conjugate prepared with EDC/NHS and washed three times was normalized (100%), and compared to the preparations performed without these activating agents (Fig. 6).

A strong decrease of the ELISA response is observed when EDC/NHS were omitted. At a concentration of 1 ng/mL of anti-BSA IgG, no hybridization occurs, probably due to the complete

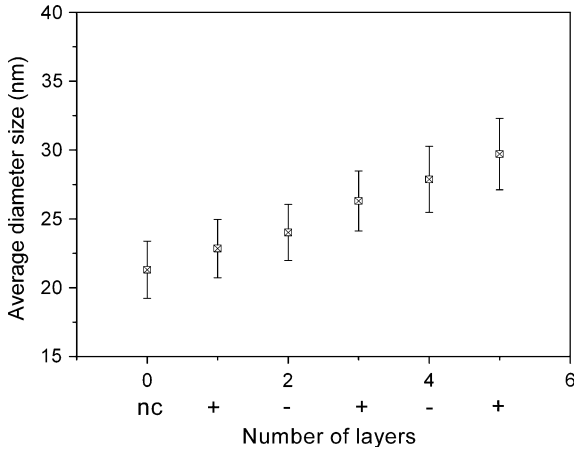

Fig. 3 Average diameter size (nm) evolution of AuNPs with the number of polyelectrolyte layers. The size has been determined from TEM images (mean ± SD; $n = 40$)

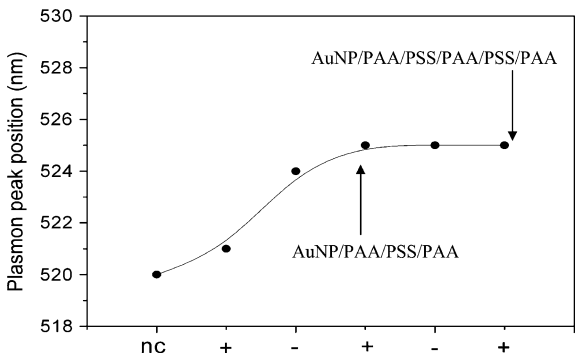

Fig. 4 Plasmon band redshift as a function of the number of polyelectrolyte layers deposited on AuNPs

Table 1 Zeta potential of uncoated gold nanoparticles (AuNP) or coated with polyallylamine (PAA) or polystyrenesulfonate (PSS)

Nanoparticle	Zeta potential (mV)
AuNP	−40
AuNP/PAA	+55
AuNP/PAA/PSS	−39
AuNP/PAA/PSS/PAA	+50
AuNP/PAA/PSS/PAA/PSS	−42
AuNP/PAA/PSS/PAA/PSS/PAA	+53

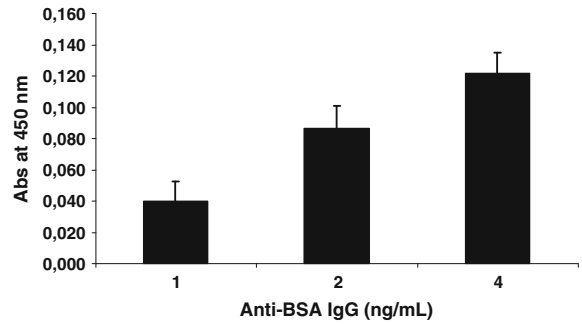

Fig. 5 ELISA response (mean ± SD; $n = 4$) of anti-BSA IgG linked to AuNP/PAA/PSS/PAA particles. The same amount of coated AuNPs reacted with 1, 2, or 4 ng/mL of anti-BSA IgG

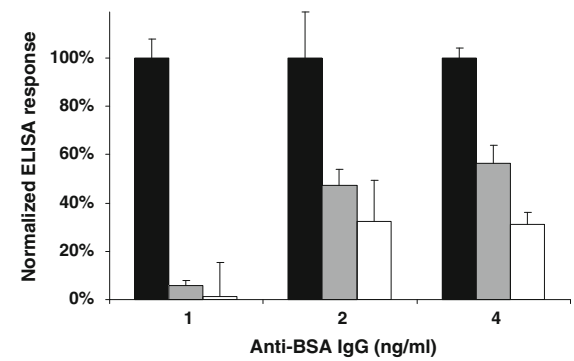

Fig. 6 ELISA response (mean ± SD; $n = 4$) of anti-BSA IgG linked or adsorbed on AuNP/PAA/PSS/PAA nanoparticles. The same amount of coated AuNPs reacted with 1, 2, or 4 ng/mL of anti-BSA IgG in the presence (*black*) or in the absence (*gray* and *white*) of EDC/NHS. The preparations were washed twice (*gray*) or three times (*black* and *white* columns). The ELISA response of the conjugate prepared in the presence of EDC/NHS is normalized and considered as 100%

Table 2 Physical parameters of uncoated and three layered AuNPs

Parameters	Uncoated AuNP	AuNP/PAA/PSS/PAA
Diameter (nm)	21.3	24.0
Surface (nm^2)	1,425	1,810
Volume (nm^3)	5,060	7,238
Density (ng/nm^3)	193×10^{-13}	
Weight (ng)	977×10^{-10}	

desorption caused by the washes. When higher concentrations of anti-BSA IgG are used, a strong decrease of the hybridization is also observed when EDC/NHS are missing. After three washes, the ELISA response in only 30% when compared to the same preparation performed with the coupling agents

EDC/NHS. These results strongly suggest that, in the presence of EDC/NHS, the anti-BSA IgG is covalently bounded to three layered AuNPs, and not adsorbed.

Taking into account the ELISA response, the gold dosage and the features of naked and three-layered AuNPs (Table 2), we estimated that the mean ratio of the number of anti-BSA IgG linked to AuNP/PAA/PSS/PAA. This ratio is 7.7 ± 1.2 for a concentration of anti-BSA-IgG of 4 ng/mL.

Discussion

Several studies have demonstrated the interest of AuNPs in cancer treatment or diagnostic. For example, AuNPs are used in photothermal therapy or as an absorber of X-rays for the treatment of solid tumors (Hirsch et al. 2003; Hainfeld et al. 2008). AuNPs have also been shown to be efficient in ovarian cancer, in multiple myeloma or in B-chronic lymphatic leukemia (Battacharya and Mukherjee 2008). Coupled to human recombinant TNF, AuNPs can be accumulated in colon carcinoma tumors where they release the cytotoxic TNF (Paciotti et al. 2004). The strategy coupling AuNPs to antibodies targeting surface proteins specifically overexpressed in cancer cells or in angiogenesis could reduce the side-effects due to a widespread AuNPs distribution including healthy tissues and organs. On the other hand, the high concentration of this bioconjugate in the tumoral tissue could allow reducing the administered dose of AuNPs for a similar therapeutic efficacy. So, AuNPs were coupled to antibodies targeting biomarkers such as EGFR (El-Sayed et al. 2005) or HER2 (Loo et al. 2005). In this study, we described a simple and reliable method to coat LbL AuNPs with ionic polymers which can be further covalently coupled to an antibody directed to an antigen overexpressed in cancer cell or angiogenesis. The successful binding of the anti-BSA-IgG monoclonal antibody shows that our method can be extended to other antibodies known to targeting specific proteins overexpressed in cancer cells and endothelial cells resulting from the angiogenesis process. Moreover, each gold nanocluster of the bioconjugate can be doped with radionuclides used for cancer treatment or imaging. In this approach, the nanocluster coupled to an antibody can contain many more radioactive atoms than an antibody directly associated to a radioactive atom in a 1:1 ratio (Bouchat et al. 2007).

Acknowledgment This study is supported by Walloon Region (Targan Project, grant 516071). C Michiels is a Research Associate of the Belgian FNRS.

References

Artemov D, Mori N, Okollie B, Bhujwalla ZM (2003) MR molecular imaging of the Her-2/neu receptor in breast cancer cells using targeted iron oxide nanoparticles. Magn Reson Med 49:403–408

Baptista P, Pereira E, Eaton P, Doria G, Miranda A, Gomes I, Quaresma P, Franco R (2008) Gold nanoparticles for the development of clinical diagnosis methods. Anal Bioanal Chem 391:943–950

Battacharya R, Mukherjee P (2008) Biological properties of "naked" metal nanoparticles. Adv Drug Deliv Rev 60:1289–1306

Bawarski WE, Chidlowsky E, Bharali DJ, Mousa SA (2008) Emerging nanopharmaceuticals. Nanomed Nanotechnol Biol Med 4:273–282

Bouchat V, Nuttens VE, Lucas S, Michiels C, Masereel B, Feron O, Gallez B, Vander Borght T (2007) Radioimmunotherapy with radioactive nanoparticles: first results of dosimetry for vascularized and necrosed solid tumors. Med Phys 34:4504–4513

Bucak S, Jones DA, Laibinis PE, Hatton TA (2003) Protein separations using colloidal magnetic nanoparticles. Biotechnol Prog 19:477–484

Buijs J, Lichtenbelt JW, Norde W, Lyklema J (1995) Adsorption of monoclonal IgGs and their F(ab′)2 fragments onto polymeric surfaces. Colloids Surf B Biointer 5:11–23

Cao YC, Jin R, Nam JM, Thaxton CS, Mirkin CA (2003) Raman dye-labeled nanoparticle probes for proteins. J Am Chem Soc 125:14676–14677

Caruso F (2001) Nanoengineering of particle surfaces. Adv Mater 13:11–22

Caruso F, Niikura K, Furlong DN, Okahata Y (1997) Ultrathin multilayer polyelectrolyte films on gold: construction and thickness determination. Langmuir 13:3422–3426

Decher G (1997) Fuzzy nanoassemblies: toward layered polymeric multicomposites. Science 277:1232–1237

Dirieh Egueh AN, Lakard B, Fievet P, Lakard S, Buron C (2010) Charge properties of membranes modified by multilayer polyelectrolyte adsorption. J Colloid Interface 344:221–227

El-Sayed IH, Huang X, El-Sayed MA (2005) Surface plasmon resonance scattering and absorption of anti-EGFR antibody conjugated gold nanoparticles in cancer diagnostics: applications in oral cancer. Nano Lett 5:829–834

Forbes ZG, Yellen BB, Barbee KA, Friedman G (2003) An approach to targeted drug delivery based on uniform magnetic fields. IEEE Trans Magn 39:3372–3377

Fortina P, Kricka LJ, Graves DJ, Park J, Hyslop T, Tam F, Halas N, Surrey S, Waldman SA (2007) Applications of

nanoparticles to diagnostics and therapeutics in colorectal cancer. Trends Biotechnol 25:145–152

Gittins DI, Caruso F (2000) Multilayered polymer nanocapsules derived from gold nanoparticle templates. Adv Mater 12:1947–1949

Gittins DI, Caruso F (2001) Tailoring the polyelectrolyte coating of metal nanoparticles. J Phys Chem B 105:6846–6852

Hainfeld JF, Dilmanian FA, Slatkin DN, Smilowitz HM (2008) Radiotherapy enhancement with gold nanoparticles. J Pharm Pharmacol 60:977–985

Hirsch LR, Stafford RJ, Bankson JA, Sershen SR, Rivera B, Price RE, Hazle JD, Halas NJ, West JL (2003) Nanoshell-mediated near-infrared thermal therapy of tumors under magnetic resonance guidance. Proc Natl Acad Sci USA 100:13549–13554

Hofman-Caris CHM (1994) Polymers at the surface of oxide nanoparticles. New J Chem 18:1087–1094

Khlebtsov NG, Dykman LA (2010) Optical properties and biomedical applications of plasmonic nanoparticles. J Quant Spectrosc Radiat Transf 111:1–35

Loo C, Lowery A, Halas N, West J, Drezek R (2005) Immunotargeted nanoshells for integrated cancer imaging and therapy. Nano Lett 5:709–711

Maggon K (2007) Monoclonal antibody "gold rush". Curr Med Chem 14:1978–1987

Mayya KS, Schoeler B, Caruso F (2003) Preparation and organization of nanoscale polyelectrolyte-coated gold nanoparticles. Adv Funct Mater 13:183–188

Mulvaney P (1996) Surface plasmon spectroscopy of nanosized metal particles. Langmuir 12:788–800

Paciotti GF, Myer L, Weinreich D, Goia D, Pavel N, McLaughlin RE, Tamarkin L (2004) Colloidal gold: a novel nanoparticle vector for tumor directed drug delivery. Drug Deliv 11:169–183

Radwan SH, Azzazy HM (2009) Gold nanoparticles for molecular diagnostics. Expert Rev Mol Diagn 9:511–524

Schneider G, Decher G (2004) From functional core/shell nanoparticles. Prepared via layer-by-layer deposition to empty nanospheres. Nanoletters 4:1833–1839

Toda M, Itakura AN, Igarashi S, Büscher K, Gutmann JS, Graf K, Berger R (2008) Surface stress, thickness, and mass of the first few layers of polyelectrolyte. Langmuir 24:3191–3198

Wilson DS, Nock S (2002) Functional protein microarrays. Curr Opin Chem Biol 6:81–85